Progress In Electromagnetics Research M, Vol. 60, 85–92, 2017

Equivalent Circuit Analysis of Artificial Dielectric Layers

Eiichi Sano[1] and Masayuki Ikebe[2, *]

Abstract—On the basis of equivalent circuit analysis, we investigated the electromagnetic characteristics of artificial dielectric layers (ADLs) having arrays of square metal patches for the normal incidence of plane waves, where the electromagnetic wavelength ranges from $p/10$ to $p/2$ (p: period). A good agreement was obtained between measured and calculated S parameters and electromagnetic parameters (permittivity and permeability) for a fabricated ADL except at around 5.2 and 9.2 GHz. A possible cause of the discrepancy between the measured and calculated electromagnetic characteristics is discussed by investigating the electromagnetic wave propagating along the surface of the ADL. Applications of the equivalent circuit analysis to ADLs with other geometries are also discussed.

1. INTRODUCTION

Metamaterials are artificial materials that exhibit electromagnetic properties not generally found in nature. Since Pendry claims that materials with a negative refractive index can act as perfect lenses [1], metamaterials have received an enormous amount of attention and interest from both the scientific and industrial communities. Artificial dielectric layers (ADLs) — composed of arrays of metal strips embedded in an insulating material — are one of the oldest metamaterials even though the term "metamaterial" was not used at the time of their invention. Artificial dielectric layers were originally proposed in a configuration of arrays of metal plates to produce a material for microwave concave lenses with an index of refraction less than unity [2]. Since the electric dipoles in an ADL produce a large effective permittivity, microwave applications other than lens have recently been investigated. These include miniaturized resonators [3, 4], silicon substrate shielding [5, 6], and antenna backplanes [7, 8]. Periodic arrays of square metal patches are often used in ADLs for the purpose of design convenience [5–7].

For an ADL composed of a dielectric layer having two periodic arrays of square metal patches on both surfaces, where one patch array is shifted by one-half period to the other patch array, the effective permittivity in the direction of the edges of the patches is approximated by $\varepsilon_{eff} = \varepsilon_d A/t^2$, where ε_d is the permittivity of the dielectric layer, A is a quarter the area of a square patch, and t is the thickness of the dielectric layer [5, 9]. In general, the period in a periodic metamaterial is much smaller than the electromagnetic wavelength at the operating frequency. The periods in ADLs are about three orders smaller than the wavelengths [5–7]. When the period is increased to increase the ε_{eff} of an ADL, it approaches the electromagnetic wavelength, and the assumption, under which the above approximate expression is derived, may be violated. The electromagnetic behavior of ADLs is of great concern in the frequency region where the electromagnetic wavelength ranges from $p/10$ to $p/2$ (p: period of patch array).

Although numerical simulations on the basis of a finite-difference time-domain scheme or finite element method are rigorous to investigate the electromagnetic behavior of ADLs, a huge amount

Received 28 April 2017, Accepted 7 September 2017, Scheduled 9 September 2017

* Corresponding author: Masayuki Ikebe (ikebe@ist.hokudai.ac.jp).

[1] Research Center for Integrated Quantum Electronics, Hokkaido University, Sapporo 060-8628, Japan. [2] Graduate School of Information Science and Technology, Hokkaido University, Sapporo 060-0814, Japan.

of computation time is required, and intuitive grasp of the relation between the ADL structure and electromagnetic parameters (effective permittivity and permeability) is quite difficult. Although mode-expansion methods reduce computation resources, they are still complicated to handle [10, 11].

In this study, we investigate the electromagnetic characteristics of ADLs having arrays of square metal patches for the normal incidence of plane waves, where the electromagnetic wavelength ranges from $p/10$ to $p/2$. Although the electromagnetic characteristics of ADLs only for the normal incidence of plane waves were analyzed using a simple equivalent circuit, the analysis method can be extended to the electromagnetic characterization for oblique incidence of transverse electric (TE) and transverse magnetic (TM) waves by changing the impedances in the equivalent circuit in a similar manner to those described by Luukkonen et al. [12]. In Section 2, we describe the measurement and analysis methods and discuss the evaluation by using well-understood artificial magnetic conductors (AMCs). In Section 3, we analyze the electromagnetic characteristics of an ADL on the basis of a simple equivalent circuit. In Section 4, we discuss the applicable range of the equivalent circuit analysis. In the final section, we mention applications of the equivalent analysis method to ADLs with other geometries.

2. MEASUREMENT AND ANALYSIS METHODS

A vector network analyzer (Keysight Technologies, E8361C) and a pair of horn antennas (Schwarzbeck, BBHA9120C) were used to measure the scattering (S) parameters. The two-port system was calibrated using the gated reflect line calibration method (Keysight Technologies, 85071E) [13]. Fig. 1 shows a schematic view and a photograph of a fabricated ADL. The p and gap g of Cu patches were 16 and 1 mm, respectively. The patch array on the front surface was shifted by one-half period (8 mm) to the patch array on the rear surface in both x and y directions. The substrate was FR4 with a t of 1.6 mm. The wave vector of the incident plane wave was in the z-direction.Commercially available electromagnetic absorbers were placed on four edges of the fabricated ADL to avoid any electromagnetic wave radiation from the edges.

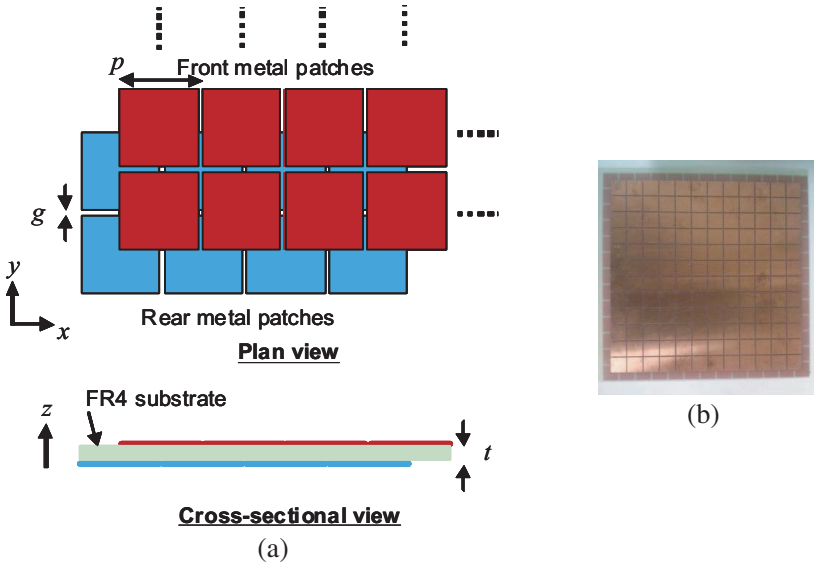

Figure 1. (a) Schematic view and (b) photograph of ADL.

Before investigating the fabricated ADL, AMCs were measured and analyzed using an equivalent circuit. An AMC is produced by replacing the rear metal patches in ADL with whole metal. The equivalent circuit of an AMC for the normal incidence of plane waves is shown in Fig. 2(a) [14]. The gap capacitance is given by

$$C_g = \alpha(p-g)\varepsilon_0 \frac{\varepsilon_d + 1}{2} \frac{K(\sqrt{1-(g/p)^2})}{K(g/p)}, \tag{1}$$

where ε_0 is the permittivity of vacuum, ε_d the relative permittivity of the FR4 substrate, K the complete elliptic integral of the first kind, and α a factor related to the finite size edge effects [14]. The characteristic impedance of an AMC is given by

$$Z = \frac{jZ_d \tan(\beta t)}{1 - \omega C_g Z_d \tan(\beta t)}, \tag{2}$$

where Z_d is the characteristic impedance of the FR4 substrate, β the wave number in the substrate, and ω the angular frequency [14].

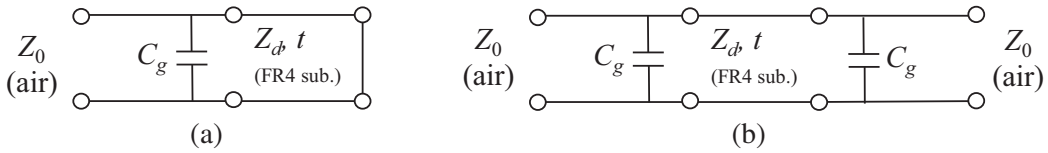

Figure 2. Equivalent circuits for (a) AMC and (b) ADL.

Two types of AMCs were measured and characterized. The periods were 3.6 and 4.8 mm, while both AMCs had a g of 0.15 mm and a t of 1.6 mm. Fig. 3 shows comparisons between measured and calculated reflection (S_{11}) phases and characteristic impedances, where the capacitance values of 0.13 and 0.21 pF used in the calculations were determined by adjusting the α in Eq. (1) to 0.55 and 0.62 for the AMCs with p of 3.6 and 4.8 mm, respectively, to fit the calculated resonant frequencies to the measured resonant frequencies. Good agreement between measured and calculated results was obtained, which showed that the validity of the measurement and analysis methods was confirmed.

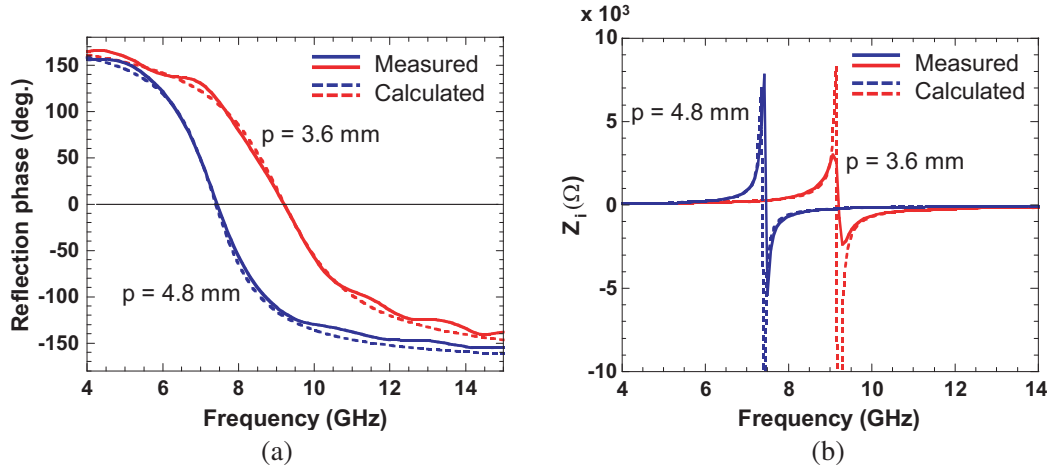

Figure 3. Comparisons between measured and calculated (a) reflection phases and (b) characteristic impedances for AMCs.

3. MEASURED AND CALCULATED RESULTS FOR ADL

A straightforward modification of the equivalent circuit for an AMC leads to an equivalent circuit for an ADL shown in Fig. 2(b). The S parameters for an ADL were converted from the cascade-connecting F matrices [15]. Fig. 4 shows comparisons between measured and calculated S parameters and reflection (S_{11}) phase, where the capacitance value of 0.54 pF used in the calculations was determined by adjusting the α in Eq. (1) to 0.58 to fit the calculated resonant frequency to the measured resonant frequency at 6.8 GHz. Good agreement between measured and calculated results was obtained. A possible cause of the discrepancy between measured and calculated S parameters at around 5 GHz is discussed in the next section.

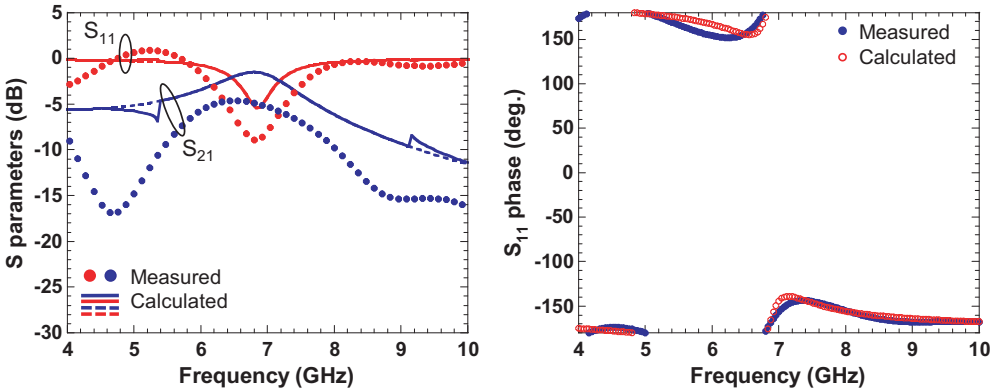

Figure 4. Comparisons between measured and calculated (a) S parameters and (b) reflection phase for ADL. Dotted lines: calculations using equivalent circuit shown in Fig. 2(b). Solid lines: calculations taking into account surface waves.

The characteristic impedance, permittivity, and permeability of the fabricated ADL were reduced from the S parameters using the expressions described in a previous study [16] (Eqs. (4)–(6) in [16]). Fig. 5 shows a comparison between measured and calculated characteristic impedance. A clear resonance was observed at 6.8 GHz. Since the reflection phase was not zero at the resonance frequency, as shown in Fig. 4(b), however, the ADL did not act as a magnetic conductor. The complex permittivity and permeability of the ADL are respectively shown in Figs. 6 and 7. (The permittivity and permeability described in as follows are meant as relative values.) The agreement between measured and calculated (represented with dotted lines) permittivity and permeability was quite good except at around 5.2 and 9.2 GHz.

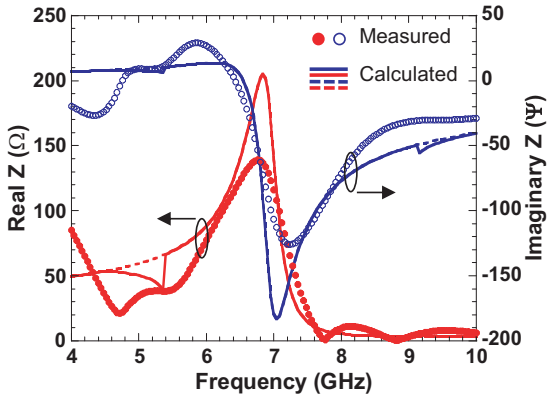

Figure 5. Comparison between measured and calculated characteristic impedance of ADL. Dotted lines: calculations using equivalent circuit shown in Fig. 2(b). Solid lines: calculations taking into account surface waves.

4. DISCUSSION

The equivalent circuit could well explain the electromagnetic characteristics of the fabricated ADL for the normal incidence of plane waves except at around 5.2 and 9.2 GHz. In this section, we discuss a possible cause of the discrepancy between measured and calculated electromagnetic characteristics (especially permittivity). To do this, the electromagnetic wave propagating along the surface of the fabricated ADL (x direction in Fig. 1(a)) was modeled using an equivalent circuit. Fig. 8 shows a unit cell composed of two parallel strip lines (each in the front metal-substrate-rear metal) and a gap

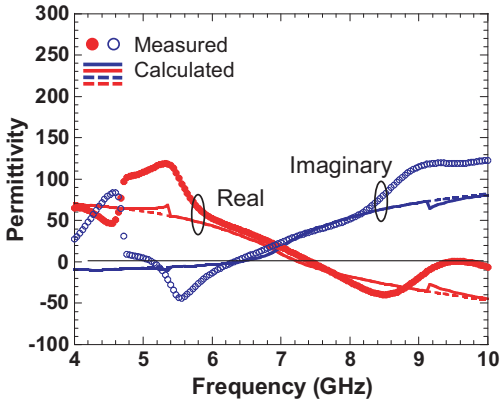

Figure 6. Comparison between measured and calculated permittivity of ADL. Dotted lines: calculations using equivalent circuit shown in Fig. 2(b). Solid lines: calculations taking into account surface waves.

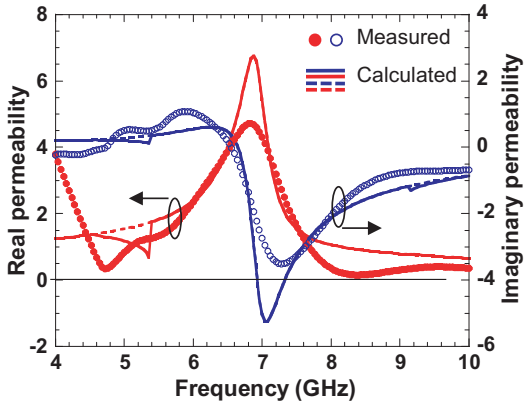

Figure 7. Comparison between measured and calculated permeability of ADL. Dotted lines: calculations using equivalent circuit shown in Fig. 2(b). Solid lines: calculations taking into account surface waves.

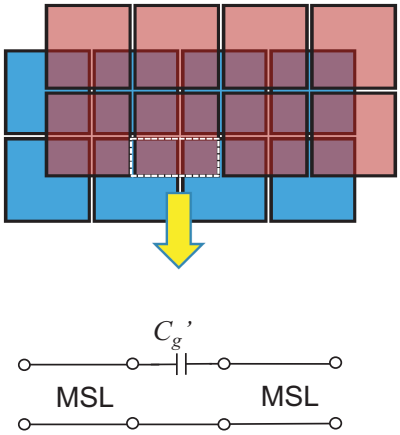

Figure 8. Equivalent circuit for electromagnetic wave propagating along the surface of ADL.

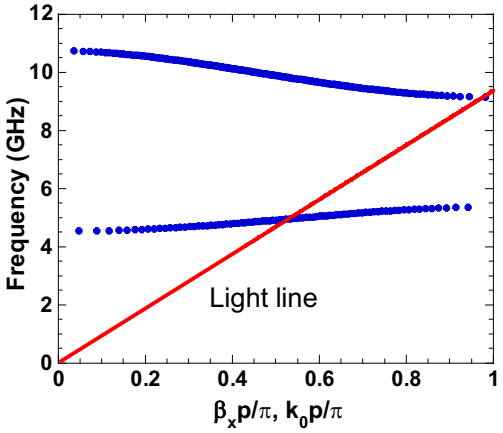

Figure 9. Calculated dispersion for wave propagating along surface of ADL, where k_0 is wave number in free space.

capacitor extracted from the ADL. Since the parallel strip line with a certain t is equivalent to a microstrip line (MSL) with $t/2$ [17], the unit cell can be modeled with two MSLs and the gap capacitor C'_g [$= C_g(p-2g)/2/(p-g)$, where C_g is given by Eq. (1)]. Each MSL had a width of 7 mm, length l of 7.5 mm, and a t of 0.8 mm. The effective permittivity ε_{eff} and characteristic impedance Z_{MSL} of the MSLs were calculated to be 3.47 and 17.3 Ω, respectively [17]. A periodic boundary condition for the unit cell leads to frequency versus wave number (dispersion) characteristics given by

$$\beta_x p = \cos^{-1}\left[\cos^2(\beta_{MSL}l) - \sin^2(\beta_{MSL}l) + \frac{\sin(\beta_{MSL}l)\cos(\beta_{MSL}l)}{Z_{MSL}\omega C'_g}\right], \tag{3}$$

where β_x is the propagation constant in the x direction and β_{MSL} the propagation constant of MSLs.

The calculated dispersion characteristics for the electromagnetic wave propagating in the x direction are shown in Fig. 9. A right-handed propagation mode appeared in the frequency region from 4.54 to 5.36 GHz, while a left-handed propagation mode appeared in the frequency region from 9.15 to 10.73 GHz. These frequency regions correspond to those where the measured electromagnetic characteristics deviated from the calculations. When a plane wave with a frequency in these regions is

incident to an ADL, a standing wave is generated on the surface of the ADL and affects the measured S parameters. The effect of this surface wave is ignored in the equivalent circuit shown in Fig. 2(b).

We then attempted to introduce the effects of the surface wave propagations in the frequency regions from 4.54 to 5.36 GHz and from 9.15 to 10.73 GHz into the equivalent circuit shown in Fig. 2(b). To do this, the propagation constant in the FR4 substrate was changed to

$$\beta_z = \sqrt{\varepsilon_d k_0^2 - \beta_x^2}, \tag{4}$$

where k_0 is the wave number in free space, and β_x is given by Eq. (3). The solid lines in Figs. 4–7 are the calculated results using the modified propagation constant. The modification qualitatively explained the experimental results. The possible cause of the quantitative discrepancy between the calculated and measured results was the imperfection of the surface wave absorption at the ADL edges.

Under the assumption that permeability equals 1.0, $\sin(\beta t) \sim \beta t$, and $\cos(\beta t) \sim 1.0$ in the low-frequency regions, a straight forward calculation leads to approximate expressions for real and imaginary permittivity of an ADL and given by

$$\varepsilon_r' = \varepsilon_d + \frac{2C_g}{\varepsilon_0 t} \tag{5}$$

and

$$\varepsilon_r'' = \omega C_g Z_0 \left(1 + 2\varepsilon_d + \frac{2C_g}{\varepsilon_0 t}\right) \approx 0, \tag{6}$$

respectively, where ε_0 is the permittivity of vacuum and Z_0 the characteristic impedance in free space. Eq. (5) gives the real permittivity of 80.2 for the ADL used in the experiments, while the electrostatic approximation ($\varepsilon_{eff} = \varepsilon_d A/t^2$) gives the real permittivity of 97. It is obvious that the difference in the permittivity values is caused by the different basis of the equivalent circuit and electrostatic approximation models.

5. APPLICATIONS TO ADLS WITH OTHER GEOMETRIES

The equivalent circuit analysis was applied to ADLs with other geometries. Fig. 10(a) shows the shape of the elemental metal patch used in the exploration of another ADL. The metal patch had four slits with each width w_s of 1 mm and length l_s of 5 mm. The ADL was composed of a 1.6-mm-thick FR4 substrate sandwiched by two metal patch arrays, the elemental patch of which had the shape shown in Fig. 10(a). To take into account the effect of the slits, three circuit elements [C_s, L_{s1}, and L_{S2} shown in Fig. 10(b)] were added to the equivalent circuit of the patch array without slits. Here $C_g'' = C_g(p - g - w_s)/(p - g)$ and $C_s = C_g l_s/(p - g)$, where C_g is given by Eq. (1). Fig. 11 shows a comparison between measured and calculated S parameters for the ADL, where L_{s1} of 1.8 nH and L_{s2} of 1.05 nH were used to match the resonances measured at around 8 and 10 GHz to the calculation. A quite good agreement between measured and calculated S parameters was obtained.

The equivalent circuit analysis was applied to ADLs with arbitrary numbers of metal layers by cascading appropriate equivalent circuits. Fig. 12(a) shows a schematic cross section of an ADL

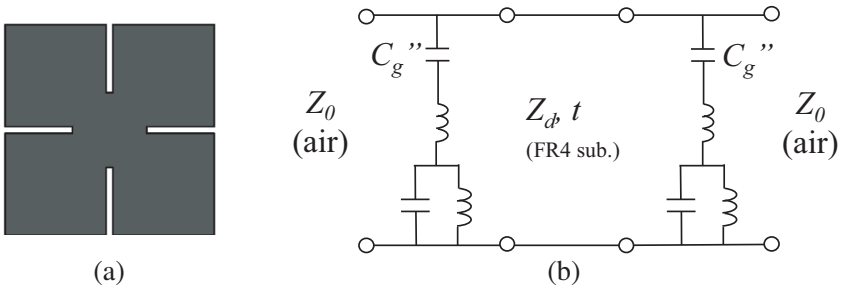

Figure 10. (a) Elemental metal patch with four slits and (b) equivalent circuit of ADL composed of FR4 substrate sandwiched by two metal patch arrays.

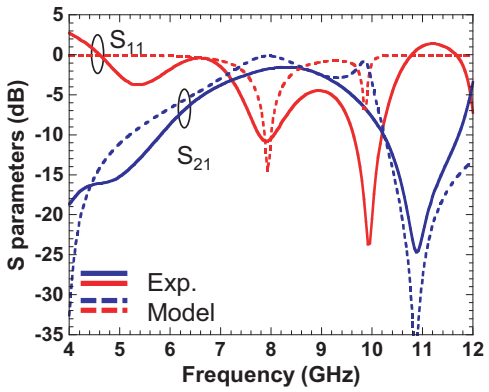

Figure 11. Measured and calculated S parameters for ADL having patches with slits.

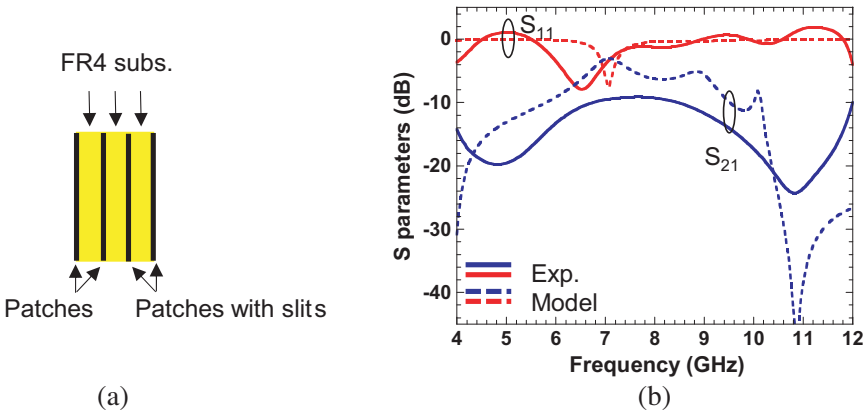

Figure 12. Measured and calculated S parameters for ADL composed of four patch layers and three FR4 layers between them. (a) Schematic cross section. (b) S parameters.

composed of four metal patch layers and three FR4 layers between them, where two metal layers had the elemental square patch shown in Fig. 1(a) and the other layers had the elemental square patch with slits shown in Fig. 10(a). The thickness of each FR4 layer was 1.6 mm. The S parameters for the ADL were calculated by connecting the equivalent circuits shown in Figs. 2(b) and 10(b) through the transmission line for the FR4 layer. Fig. 12(b) compares the measured and calculated S parameters for the ADL. Agreement was fairly good.

6. CONCLUSION

On the basis of equivalent circuit analysis, we investigated the electromagnetic characteristics of ADLs having arrays of square metal patches for the normal incidence of plane waves where the electromagnetic wavelength ranges from $p/10$ to $p/2$. A good agreement was obtained between measured and calculated S parameters and electromagnetic parameters (permittivity and permeability) for the fabricated ADL except at around 5.2 and 9.2 GHz. An equivalent circuit analysis for the electromagnetic wave propagating along the surface of the ADL revealed that these frequency regions corresponded to right-handed and left-handed propagation modes. The improved equivalent circuit model taking into account the surface wave propagation qualitatively explained the experimental results. These new findings are useful for understanding the fundamental behavior of ADLs. It was also shown that the equivalent circuit analysis was effective for ADLs with other geometries. Although the equivalent circuit analysis is inferior to full-wave numerical simulations in terms of accuracy, it is helpful to intuitively grasp the relation between the ADL structure and electromagnetic characteristics and useful for schematic design of ADLs.

REFERENCES

1. Pendry, J. B., "Negative refraction makes a perfect lens," *Physical Review Letters*, Vol. 85, 3966–3969, 2000.
2. Kock, W. E., "Metal-lens antennas," *Proceedings of the IRE*, Vol. 34, 828–836, 1946.
3. Awai, I., H. Kubo, T. Iribe, D. Wakamiya, and A. Sanada, "An artificial dielectric material of huge permittivity with novel anisotropy and its application to a microwave BPF," *IEEE MTT-S Digest*, Vol. 1, 301–304, Philadelphia, 2003.
4. Huang, D., T. La Rocca, and M.-C. F. Chang, "Low phase noise millimetre-wave frequency generation using embedded artificial dielectric," *Electronics Letters*, Vol. 43, No. 18, 983–984, 2007.
5. Ma, Y., B. Rejaei, and Y. Zhuang, "Artificial dielectric shields for integrated transmission lines," *IEEE Microwave and Wireless Component Letters*, Vol. 18, No. 7, 431–433, 2008.
6. Ma, Y., B. Rejaei, and Y. Zhuang, "Low-loss on-chip transmission lines with micro-patterned artificial dielectric shields," *Electronics Letters*, Vol. 44, No. 15, 913–914, 2008.
7. Takahagi, K. and E. Sano, "High-gain silicon on-chip antenna with artificial dielectric layer," *IEEE Transactions on Antennas and Propagation*, Vol. 59, No. 10, 3624–3629, 2011.
8. Syed, W. H. and A. Neto, "Front to back ratio enhancement of planar printed antennas by means of artificial dielectric layers," *IEEE Transactions on Antennas and Propagation*, Vol. 61, No. 11, 5408–5416, 2013.
9. Peuzin, J. C. and J. C. Gay, "Demonstration of the waveguiding properties of an artificial surface reactance," *IEEE Transactions on Microwave Theory and Technology*, Vol. 42, No. 9, 1695–1699, 1994.
10. Cavallo, D., W. H. Syed, and A. Neto, "Closed-form analysis of artificial dielectric layers — Part I: Properties of a single layer under plane-wave incidence," *IEEE Transactions on Antennas and Propagation*, Vol. 62, No. 12, 6256–6264, 2014.
11. Barzegar-Parizi, S. and B. Rejaei, "Calculation of effective parameters of high permittivity integrated artificial dielectrics," *IET Microwaves, Antennas & Propagation*, Vol. 9, No. 12, 1287–1296, 2015.
12. Luukkonen, O., C. Simovski, G. Granet, G. Goussetis, D. Lioubtchenko, A. V. Raisanen, and S. A. Tretyakov, "Simple and accurate analytical model of planar grids and high-impedance surfaces comprising metal strips or patches," *IEEE Transactions on Antennas and Propagation*, Vol. 56, No. 6, 1624–1632, 2008.
13. http://www.keysight.com/upload/cmc_upload/All/FreeSpaceSeminarRev2.pdf.
14. Mosallaei, H. and K. Sarabandi, "Antenna miniaturization and bandwidth enhancement using a reactive impedance substrate," *IEEE Transactions on Antennas and Propagation*, Vol. 52, No. 9, 2403–2414, 2004.
15. Pozar, D. M., *Microwave Engineering*, 2nd edition, John Wiley and Sons, Hoboken, NJ, 1998.
16. Smith, D. R., S. Schultz, P. Marko, and C. M. Soukoulis, "Determination of effective permittivity and permeability of metamaterials from reflection and transmission coefficients," *Physical Review B*, Vol. 65, 195104, 2002.
17. Collin, R. E., *Foundations for Microwave Engineering*, 2nd edition, McGraw-Hill, New York, NY, 1992.